DOI: 10.24850/j-tyca-2020-03-06

Articles

Effects of the blockage ratio due to hydrokinetic turbines for producing energy in irrigation channels

Efectos de la relación de bloqueo por turbinas hidrocinéticas para el aprovechamiento energético en canales de riego

Javier Martínez-Reyes[1], ORCID: https://orcid.org/0000-0002-3038-2586
Nahún Hamed García-Villanueva[2], ORCID: https://orcid.org/0000-0003-3708-9822

[1]Universidad Nacional Autónoma de México, Mexico City, Mexico, javier.martinez@posgrado.imta.edu.mx
[2]Comisión Nacional del Agua, Mexico City, Mexico, nahun.garcia@conagua.gob.mx

Correspondence author: Javier Martínez-Reyes, javier.martinez@posgrado.imta.edu.mx

Abstract

In this paper, the effect of the blockage ratio generated by the hydrokinetic turbines upon the obtainable hydraulic power in an open channel is analyzed in order to validate part of the theory related to the calculation of the maximum obtainable power by the hydrokinetic turbines, by using porous discs in an experimental open channel. This

analysis is supplemented with the study and characterization of the way in which is developed the wake, that is produced downstream, and the experimental results are compared with those of a one-dimensional numerical model.

During the development of the experimental study, three different blockage ratios were analyzed, for which the hydraulic variables were kept fixed in the experimental open channel. Under these conditions, in order to characterize the behavior of the flow and obtain the components of the instantaneous velocity an acoustic Doppler velocimeter was utilized; and to measure the hydrodynamic thrust on the discs a load cell was employed.

Among the main results it was found that the velocity in the zone of the far wake has a 90% recovery at approximately 12 diameters downstream from the disc. It is noteworthy that, at this distance, the turbulent intensity was 8%, while the mean turbulence intensity in the section of the open channel where the porous discs are located, before its placement, it was 5.7%.

The power coefficients obtained for the different blockage ratios show a 59% increase between the lowest blockage ratio B_1 = 0.090 and the highest B_3 = 0.197. The differences between the power coefficients of the experimental tests and the maximums obtained with the one-dimensional theory are 19.45% for the case of B_1 = 0.090; 4.13% for B_2 = 0.156; and 0.84% for B_3 = 0.197. In general, according to the one-dimensional theory, using a blockage ratio of around 0.20 the values of the power coefficient are similar to the maximums expected, and using

Tecnología y ciencias del agua, ISSN 2007-2422, 11(3), 190-235. DOI: 10.24850/j-tyca-2020-03-06

lower values than 0.10, this coefficient falls by around 20% compared with the maximum theoretical coefficient.

Keywords: open channel flow, thrust coefficient, power coefficient, porous disc, energy, blockage ratio, hydrokinetic turbines.

Resumen

Con el fin de validar parte de la teoría asociada con el cálculo de la potencia máxima aprovechable por turbinas hidrocinéticas mediante el uso de discos porosos en un canal experimental, se analiza el efecto de la relación de bloqueo que generan las turbinas sobre la potencia hidráulica aprovechable en un canal. Dicho análisis se complementa con el estudio y caracterización de la forma en que se desarrolla la estela que se produce hacia aguas abajo y se comparan los resultados experimentales con los de un modelo numérico unidimensional.

Durante el desarrollo del estudio experimental se analizaron tres relaciones de bloqueo, para lo cual se mantuvieron fijas las variables hidráulicas en el canal experimental. Bajo estas condiciones, para caracterizar el comportamiento del flujo y obtener las componentes de la velocidad instantánea, se utilizó un velocímetro acústico Doppler, y para medir el empuje hidrodinámico sobre los discos se empleó una celda de carga.

Entre los principales resultados se encontró que la velocidad, dentro de la estela lejana, presenta una recuperación de 90% en aproximadamente 12 diámetros aguas abajo del disco. Es de resaltar que a esa distancia la intensidad de turbulencia fue de 8%, mientras que la

intensidad de turbulencia media en la sección del canal donde se ubican los discos porosos antes de su colocación era de 5.7%.

Los coeficientes de potencia obtenidos para las distintas relaciones de bloqueo presentan un incremento de 59% entre la relación de bloqueo más baja B_1 = 0.090 y la más alta B_3 = 0.197. Las diferencias entre los coeficientes de potencia de las pruebas experimentales y de los máximos obtenidos con la teoría unidimensional son de 19.45% para el caso de B_1 = 0.090; 4.13% para B_2 = 0.156; y 0.84% para B_3 = 0.197. Así, y en términos generales, se encontró que con una relación de bloqueo del orden de 0.20, los valores del coeficiente de potencia se asemejan a los máximos esperados de acuerdo con la teoría unidimensional, y que con valores inferiores a 0.10 de esta relación de bloqueo, dicho coeficiente cae alrededor de un 20% con respecto al máximo teóricamente esperado.

Palabras clave: canal, coeficiente de arrastre, coeficiente de potencia, disco poroso, energía, relación de bloqueo, turbinas hidrocinéticas.

Received: 13/12/2018
Accepted: 12/09/2019

Introduction

Mexico has an extensive network of irrigation canals, whose infrastructure corresponds to 49 160 km of canals, whereof 12 643 km are primary and

36 517 km secondary, and 47 percent of the total has concrete lining (Lomelí & Álvarez, 2014). The hydraulic energy, especially that associated with the velocity of water, can be utilized to generate electricity in these canals by using hydrokinetic turbines, which obtain the most efficient use of the flow velocity. The installation of this type of turbine does not require large investments in engineering works, and the turbines can be localized in close sites to the place where energy is needful, avoiding with that the installation of large power lines.

The theory of actuator disc is the mathematical representation of a turbine in fluid dynamics calculations. In this theory, the load on a real rotor is replaced by a distributed pressure on an infinitely thin permeable disc with the same diameter. In its more elemental representation, this load is uniform and normal, with the disc placed in an axial flow, in other words, perpendicular to the flow direction (Okulov & van Kuik, 2012).

The one-dimensional theory to calculate the maximum obtainable power in channels has been studied by different authors, whom employ the actuator disc concept in order to emulate the blockage effects produced by the turbines (Garrett & Cummins, 2007; Houlsby, Draper, & Oldfield, 2008; Whelan, Graham, & Peiró, 2009), being Houlsby *et al*. (2008) whom propose the most complete model, to the extent that it considers the increase in the depth upstream of the disc and it enables to use high Froude numbers. These authors prove that whether the blockage effects of turbines and close channel boundaries (constrained flow) are considered, the power coefficient can exceed the Betz limit that is $C_{p\max} = 0.593$, in other words, the maximum limit of obtainable power of turbines in unconstrained flow can increase.

Tecnología y ciencias del agua, ISSN 2007-2422, 11(3), 190-235. DOI: 10.24850/j-tyca-2020-03-06

Furthermore, some authors have carried out studies of the influence of the blockage ratio in the turbine efficiency and the behavior of the far wake by using computational fluid dynamics (CFD) models (Chime & Malte, 2014). Others have developed tests in experimental channels with rectangular fences or arrays of porous discs in the cross-section of the channel (Myers & Bahaj, 2012). Nonetheless, experimental studies with an isolated disc that represents a single turbine in a channel with different blockage ratios have not been developed yet.

The study of behavior of the far wake downstream of the hydrokinetic turbines enables to know the optimum distance between turbines in an array of turbines placed in series. Furthermore, it makes possible to characterize the effect of the blockage ratio in the energy harnessing. This is fundamental to establish the bases for the dimensioning and location of this type of turbines in canals.

This study has as objective to analyze and quantify the effect of the blockage ratio generated by hydrokinetic turbines in the obtainable hydraulic power in a canal. Hence, the experimental results using porous discs are compared with those obtained in a one-dimensional numerical model in order to calculate the maximum obtainable power. Moreover, the way in which is developed the wake generated downstream is characterized, by analyzing the velocity recovery and turbulence intensity curves. This can be used as a guidance tool on energy potential exploitation in irrigation canals using hydrokinetic turbines, inasmuch as this will enable us to select both its dimensions and its optimum location, and in some cases to establish the minimum distance between turbines when these are placed in series.

Tecnología y ciencias del agua, ISSN 2007-2422, 11(3), 190-235. DOI: 10.24850/j-tyca-2020-03-06

Materials and methods

Tests were carried out in an experimental facility in order to examine the behavior of the flow in channels and the maximum performance of turbines for different scenarios of blockage employing porous discs. Furthermore, the changes on the far wake region by effect of the inclusion of porous discs in the fluid, and the resultant and possible manifestation of surface gravity waves in channels were analyzed.

Calculation of the power coefficient of an axial flow hydrokinetic turbine as a function of the blockage ratio

The one-dimensional theory was used in order to calculate the theoretical power coefficient of a hydrokinetic turbine as a function of the blockage ratio of the channel (Houlsby *et al*., 2008). Part of the theoretical approach to calculate such coefficient is presented below.

A representation of a turbine in an open channel using the actuator disc concept is shown in Figure 1, where five sections are identified: (1) far upstream of the turbine, (2) immediately upstream of the turbine, (3) immediately downstream of the turbine,(4) sufficiently far downstream from the turbine where the pressure can be treated as uniform again

Tecnología y ciencias del agua, ISSN 2007-2422, 11(3), 190-235. DOI: 10.24850/j-tyca-2020-03-06

(although the velocity is not) and (5) sufficiently far downstream for that the flow has uniform velocity (Houlsby *et al*., 2008).

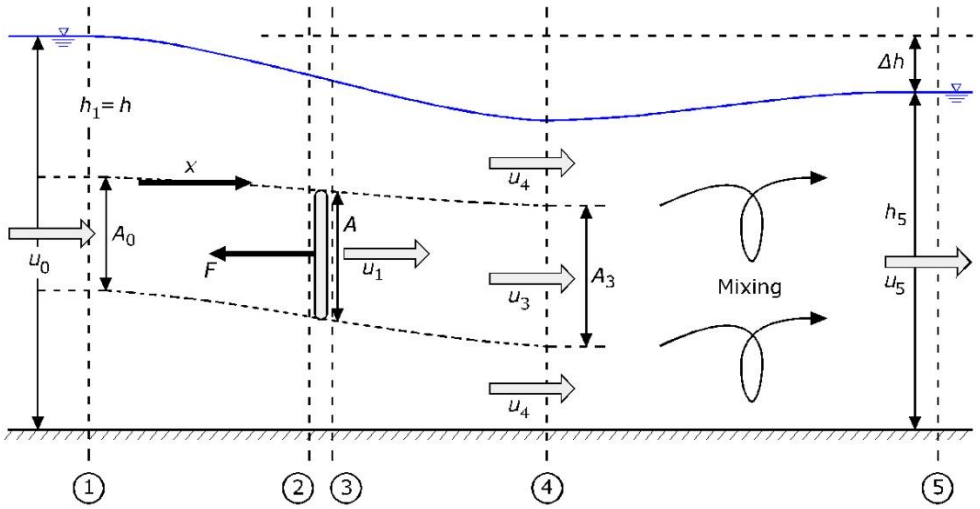

Figure 1. Representation of a turbine in an open channel. Source: (Houlsby *et al*., 2008).

In the sections 1, 4 and 5 it is assumed that the pressure is hydrostatic, the dimensions downstream of the flow are not fixed, but there is relationship between dimension and velocity, and between dimension and pressure force (Houlsby *et al*., 2008).

The development of equations 1 to 11 have been taken from Houlsby *et al*. (2008).

Applying the Bernoulli equation in the sections 1 and 4 (in the bypass flow region), as well as between the sections upstream and downstream of the turbine, and the equilibrium condition of forces in the turbine, we get:

Tecnología y ciencias del agua, ISSN 2007-2422, 11(3), 190-235. DOI: 10.24850/j-tyca-2020-03-06

$$F = \frac{\rho u_0^2 B b h_1}{2}(\tau^2 - \alpha^2) \quad (1)$$

Where:

B: blockage ratio.

b: width of the open channel in m.

h_1: hydrostatic head in the section 1 in m.

F: hydrodynamic thrust force in the turbine/disc in N.

u_o: mean velocity of the flow upstream from the turbine/disc in m/s.

α: constant that represent the relationship between the mean velocity of the flow in the wake downstream of the turbine/disc u_3 with the velocity u_0.

ρ: water density in kg/m^3.

τ: constant that represent the relationship between the mean velocity of the flow outside the wake of the stream tube (in the bypass flow region) downstream of the localization of the turbine/disc u_4, with the velocity u_0.

Applying the momentum equation between the sections 1 and 4:

$$\frac{1}{2}g(h_1^2 - h_4^2) - Bh_1\frac{u_0^2}{2}(\tau^2 - \alpha^2) = u_0^2 h_1 B\beta(\alpha - 1) + u_0^2 h_1(1 - B\beta)(\tau - 1) \quad (2)$$

where:

g: acceleration due to gravity in m/s^2.

h_4: hydrostatic head in the section 4 in m.

β: constant that relates the mean velocity of the flow in the location of the turbine/disc u_1 with the velocity u_0.

Furthermore, using the continuity relation:

Tecnología y ciencias del agua, ISSN 2007-2422, 11(3), 190-235. DOI: 10.24850/j-tyca-2020-03-06

$$h_4 = Bh_1\frac{\beta}{\alpha} + h_1\frac{(1-B\beta)}{\tau} \quad (3)$$

and developing some combinations and algebraic rearrangements are obtained the next equations:

$$B\beta\frac{(\tau-\alpha)}{\alpha\tau} = \frac{\tau-1}{\tau} - \frac{u_0^2}{2gh_1}(\tau^2-1) \quad (4)$$

and:

$$B\beta(\tau-\alpha)\left(4+\frac{(\tau^2-1)}{\alpha\tau}\right) = 2B(\tau^2-\alpha^2) + \frac{(1-\tau)^3}{\tau} \quad (5)$$

Isolating β from 5 gives the solution:

$$\beta = \frac{2(\tau-\alpha) - \frac{(\tau-1)^3}{B\tau(\tau-\alpha)}}{4+\frac{(\tau^2-1)}{\alpha\tau}} \quad (6)$$

The Froude number upstream is:

$$F_r = \frac{u_0}{\sqrt{gh_1}} \quad (7)$$

Dividing 6 and 4 to eliminate β and after an algebraic reorganization, an equation of fourth order in τ is gotten:

$$\frac{F_r^2}{2}\tau^4 + 2\alpha F_r^2\tau^3 - (2-2B+F_r^2)\tau^2 - (4\alpha+2\alpha F_r^2-4)\tau + \left(\frac{F_r^2}{2}+4\alpha-2B\alpha^2-2\right) = 0 \quad (8)$$

Tecnología y ciencias del agua, ISSN 2007-2422, 11(3), 190-235. DOI: 10.24850/j-tyca-2020-03-06

The thrust coefficient C_T is defined as:

$$C_T = \frac{F}{\frac{1}{2}\rho B b h_1 u_0^2} \quad (9)$$

Combining 1 with 9 gives:

$$C_T = (\tau^2 - \alpha^2) \quad (10)$$

The power coefficient C_P is expressed as:

$$C_P = \frac{P}{\frac{1}{2}\rho B b h_1 u_0^3} \quad (11)$$

Moreover, the power extracted from the flow by the turbine is $P = Fu_1$ (Whelan *et al*., 2009) and making a sustitution in 11 gives:

$$C_P = \beta(\tau^2 - \alpha^2) \quad (12)$$

The parameter employed regularly to represent the velocity loss in the zone of the turbine is the axial induction factor (Whelan *et al*., 2009):

$$a = 1 - \frac{u_1}{u_0} \quad (13)$$

where:
a: axial induction factor.

And given that $u_1 = \beta u_0$ is obtained:

Tecnología y ciencias del agua, ISSN 2007-2422, 11(3), 190-235. DOI: 10.24850/j-tyca-2020-03-06

$$a = 1 - \beta \tag{14}$$

The procedure for calculating the power coefficient and its respective blockage rate by using the one-dimensional theory is presented by Houlsby *et al*. (2008), and it is shown below:

a) Values of ρ, g and h_1 are specified, and it is assumed that h_1 is the depth in the channel.

b) The Froude number upstream is calculated with the equation (7).

c) The blockage rate B is calculated with the equation (15):

$$B = \frac{A}{b\, h_1} \tag{15}$$

where:

A: area of the turbine/disc in m^2.

d) A set of values of α is proposed, which must be between the range $0 \leq \alpha \leq 1$, and for every one of them τ is obtained using the solution of the equation (8).

e) β is calculated with the equation (6), such as $\tau > 1$ and $1 > \beta > \alpha$.

f) The thrust coefficient C_T is calculated with the equation (10).

g) The power coefficient C_p is calculated using the equation (12). Then, a curve of C_p vs a is generated with these values, and the maximum value of C_p is selected to obtain the maximum power coefficient C_{pmax}.

Tecnología y ciencias del agua, ISSN 2007-2422, 11(3), 190-235. DOI: 10.24850/j-tyca-2020-03-06

Experimental tests with various blockage ratios

The tests were developed in a rectangular section open channel with a length of 5.0 meters, width of 0.245 meters and height of 0.5 meters (see Figure 2).

Figure 2. Rectangular section experimental channel.

The porous discs placed into the channel were made of polylactic acid (PLA) by using a 3D printer. Those have a 4 mm thickness and a 34% porosity, which is the relationship between open and closed area of the disc. Its pores or holes are 3 mm in diameter and are 5.3 mm equidistant from each other, it is worth emphasizing that this configuration has already been used in other experimental studies (Xiao, Duan, Sui, & Rösgen, 2013).

In this study, a separation of 0.2 *h* (0.06 m) between the bottom base of the porous discs and the bed of the channel was adopted, where

Tecnología y ciencias del agua, ISSN 2007-2422, 11(3), 190-235. DOI: 10.24850/j-tyca-2020-03-06

h represents the depth of the channel. That separation ensures that the disc is placed in the sufficiently far zone from the bed, in other words, in regions where velocity gradients are not high, and consequently there are not great variations with respect to the mean velocity of the flow (Figure 3).

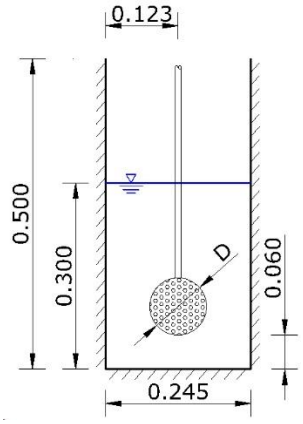

Figure 3. Location of the porous disc in the cross-sectional area of the experimental channel.

The 37 l/s flow rate corresponds to the maximum flow rate that can flow through the experimental channel. The tests were carried out using three porous discs of different diameter, making it possible to perform studies of the flow for several blockage ratios. By using the one-dimensional analysis proposed by Houlsby *et al*. (2008), the power coefficient C_p was calculated for several values of axial induction factor a of a hydrokinetic turbine of diameter equivalent to the actuator disc. The hydraulic conditions and diameters used are indicated in Table 1.

Tecnología y ciencias del agua, ISSN 2007-2422, 11(3), 190-235. DOI: 10.24850/j-tyca-2020-03-06

Table 1. Hydraulic and geometrical conditions to calculate the power coefficient.

Variable	Value	Units
ρ	998.2	kg/m^3
h	0.265	m
b	0.245	m
u_o	0.570	m/s
Fr	0.354	
D_1	0.092	m
D_2	0.121	m
D_3	0.136	m

The smaller porous disc with diameter of 92.0 mm has a low blockage ratio and has been used in experimental tests of other authors (Xiao *et al*., 2013). The greater disc with diameter of 135.7 mm provided the greatest blockage ratio, with which the one-dimensional theory proposed by Houlsby *et al*. (2008) could be verified; that of intermediate diameter, 120.8 mm in diameter, was selected seeking that the curve of power coefficient versus axial induction factor was equidistant from the two curves associated with the previous discs (see Figure 4).

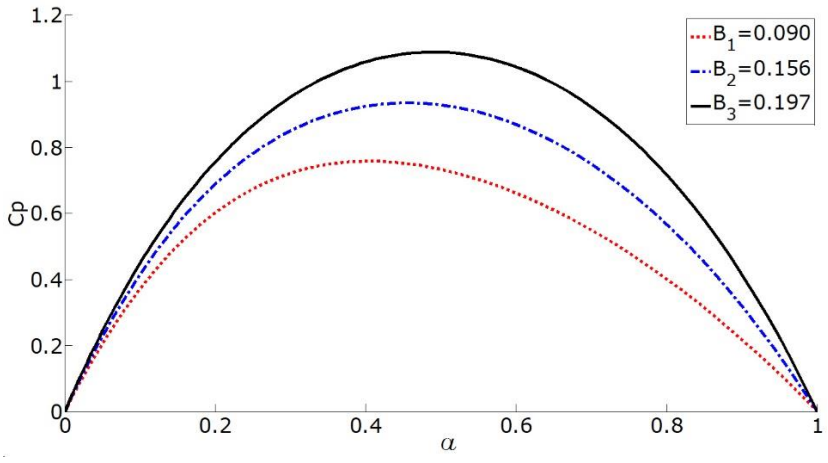

Tecnología y ciencias del agua, ISSN 2007-2422, 11(3), 190-235. DOI: 10.24850/j-tyca-2020-03-06

Figure 4. Power coefficient C_p versus axial induction factor a for experiments, h = 0.265 m.

The porous discs made with D_1 = 92 mm, D_2 = 120.8 mm and D_3 = 135.7 mm diameters are shown in Figure 5.

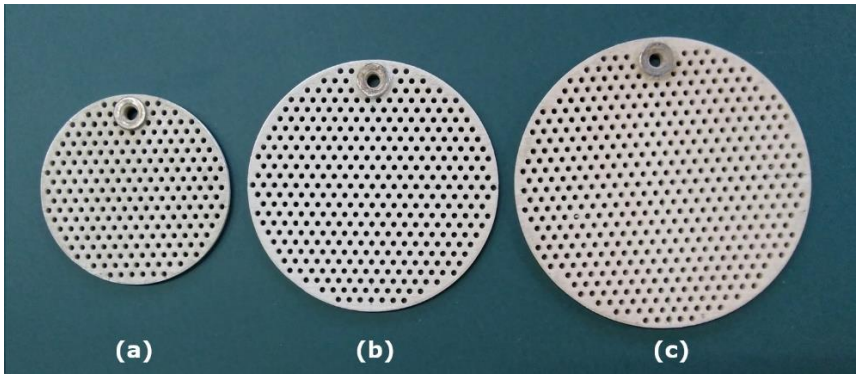

Figure 5. Diameter of porous discs: a) D_1 = 92.0 mm; b) D_2 = 120.8 mm, and c) D_3 = 135.7 mm.

In the previous tests for the discs of different diameter, with the same hydraulic conditions indicated in Table 1, and using the porous discs with D_1 = 92.0 mm and D_2 = 120.8 mm, the surface gravity waves were not notoriously visible downstream of the disc, the contrary happened with the disc of D_3 = 135.7 mm inasmuch as the phenomenon was clearly seen (Figure 6).

Tecnología y ciencias del agua, ISSN 2007-2422, 11(3), 190-235. DOI: 10.24850/j-tyca-2020-03-06

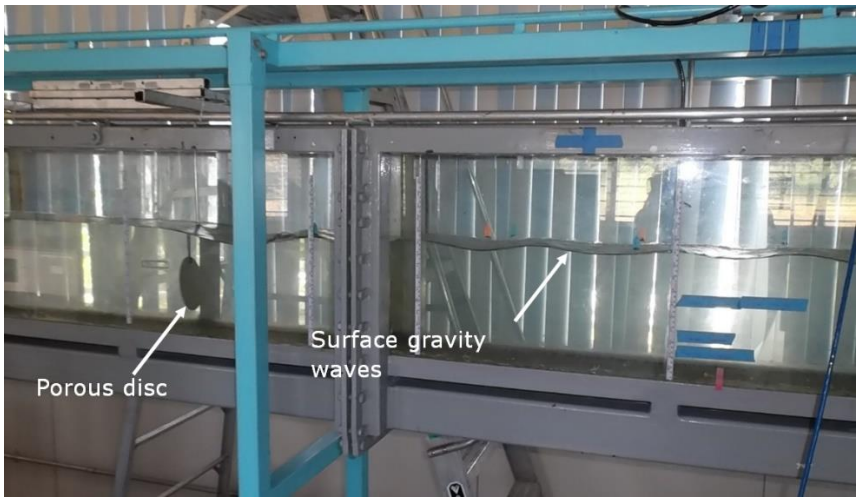

Figure 6. Surface gravity waves using the porous disc of D_3 = 135.7 mm.

Owing to the previously exposed the depth in the channel was increased, preserving the flow rate used. Thus, the new conditions with which the experiments were carried out again are shown in Table 2.

Table 2. Hydraulic conditions to calculate the power coefficient with various blockage ratios, increasing the depth in the channel.

Variable	Value	Units
ρ	998.2	kg/m^3
h	0.300	m
b	0.245	m
u_o	0.503	m/s
Fr	0.293	
D_1	0.092	m
D_2	0.121	m
D_3	0.136	m

The new results, which are derived from the application of the one-dimensional theory for the three discs, show in the best case that it is

Tecnología y ciencias del agua, ISSN 2007-2422, 11(3), 190-235. DOI: 10.24850/j-tyca-2020-03-06

possible to increase the power coefficient to $C_{p\max} = 0.985$ with the disc of $D_3 = 135.7$ mm and the blockage ratio $B_3 = 0.197$. For the disc with $D_1 = 92.0$ mm diameter and blockage ratio $B_1 = 0.090$, the maximum power coefficient gave $C_{p\max} = 0.732$, that is a higher value than the Betz limit ($C_{p\max} = 0.593$). In the case of the disc with $D_2 = 120.8$ mm diameter and blockage ratio $B_2 = 0.156$, the power coefficient is close to $C_{p\max} = 0.872$, being an average magnitude between those of the two previous maximum power coefficients (Figure 7 and Table 3).

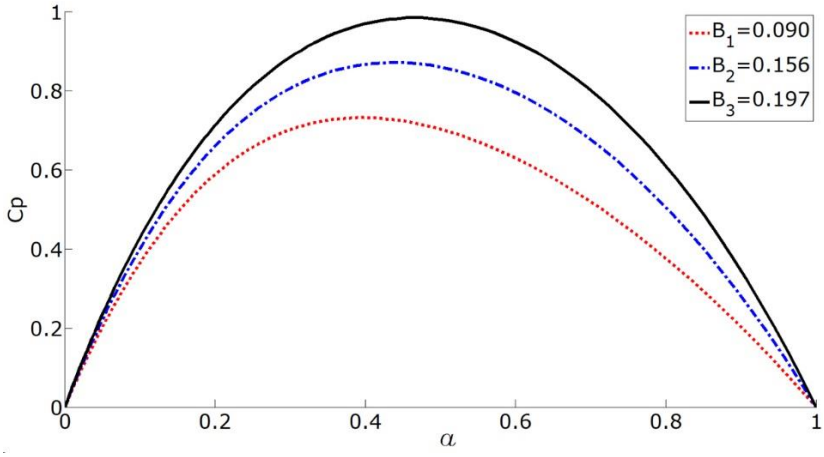

Figure 7. Power coefficient C_p versus axial induction factor a for the experiments in the experimental channel.

Table 3. Maximum power coefficient for various blockage ratios using the one-dimensional theory proposed by Houlsby *et al*. (2008).

Diameter of disc mm	Blockage ratio B	Axial induction factor a	Maximum power coefficient $C_{p\max}$
92.0	0.0904	0.399	0.732

Tecnología y ciencias del agua, ISSN 2007-2422, 11(3), 190-235. DOI: 10.24850/j-tyca-2020-03-06

120.8	0.1564	0.440	0.872
135.7	0.1976	0.466	0.985

In each case, velocity profiles were analyzed in the vertical direction at the mid-width of the channel, with separations of 3, 6, 9, 12 and 15 diameters downstream from the disc.

An acoustic Doppler velocimeter (ADV) was employed to measure the components of the instantaneous velocity in the directions (x, y, z), with a spacing in the vertical of approximately 1 mm, and a total length of measurement volume of 1 cm. In order to reduce the time employed in the measurements, these were performed in interleaved intervals: 1 cm with data and 1 cm with no data. The sampling frequency was 100 Hz with a total measurement time of 30 seconds, having thus a total of 3000 samples in each point of analysis (each millimeter). The profile of velocities starts from 0.60 cm, taking as reference the bed of the channel, to a height of 23.5 cm.

Before the interpretation and analysis of the data obtained with the ADV, outliers were removed in the points by using the method proposed by Goring and Nikora (2002), and modified by Mori, Suzuki and Kakuno (2007).

Recovery of the velocity in the far wake

When a turbine is installed in series, it is important to know the minimum distance at which is advisable to install the other turbine downstream

Tecnología y ciencias del agua, ISSN 2007-2422, 11(3), 190-235. DOI: 10.24850/j-tyca-2020-03-06

(Xiao *et al*., 2013). This is relevant to maximize the use of available space, without affecting significantly its performance. In this regard, among the main factors that influence the power generated by the hydrokinetic turbines are: the velocity of the flow and the turbulence intensity in the zone where the turbine is located (Maganga, Germain, King, Pinon, & Rivoalen, 2010). For this reason, it is important to know the effect of increasing the blockage ratio both in the velocity recovery in the far wake and in its respective turbulence intensity. In this study, a set of tests was carried out in the experimental channel in order to identify these elements.

The discs with the characteristics included in Table 2 were studied in order to know the velocity recovery in the far wake using various blockage ratios. Each disc was installed 2.0 m from the channel entrance, just in the mid-width and 6 cm from the bed. The velocity profiles were measured at the mid-width and in the vertical direction, inasmuch as this zone is the most convenient to analyze the velocity and turbulence intensity recovery effect in the wake, due to it is the worst condition presented in the wake cone.

As mentioned above, the flow rate Q = 37 l/s with the depth of 0.3 m were used, arising a mean velocity in the flow of u_0 = 0.503 m/s, Froude number Fr = 0.293, and the mean turbulence intensity in the cross-section gave IT = 5.7%. The Reynolds numbers as a function of the disc diameter were Re_1 = 46 276 for D_1 = 92.0 mm, Re_2 = 60 762 for D_2 = 120.8 mm and Re_3 = 68 257 for D_3 = 135.7 mm.

The Reynolds number is defined by Xiao *et al*. (2013) as:

$$Re = \frac{u_0 \, D}{\nu} \qquad (16)$$

Tecnología y ciencias del agua, ISSN 2007-2422, 11(3), 190-235. DOI: 10.24850/j-tyca-2020-03-06

where:

D: diameter of the porous disc in m.

Re: Reynolds number (adimensional).

ν: kinematic viscosity of water in m^2/s.

Calculation of the turbulence intensity

The turbulence intensity is a scale that characterizes the turbulence. It is expressed as a percentage, and it can be represented with the equation (17), according to Panton (2005).

$$TI = 100 \cdot \frac{\sqrt{\frac{1}{3}\left(\overline{u'^2}+\overline{v'^2}+\overline{w'^2}\right)}}{u_0} \qquad (17)$$

where:

TI: turbulence intensity in %.

u', v' y w': velocity fluctuation components in the directions *x*, *y*, *z* respectively, in m/s.

The mean turbulence intensity inherent in the channel can be obtained from the data of the velocities profiling in the vertical direction. Superposing the series of profiling generated using the data obtained with the acoustic Doppler velocimeter ADV on the turbulence intensity graphs, some patterns do not correspond to that expected in the physical

Tecnología y ciencias del agua, ISSN 2007-2422, 11(3), 190-235. DOI: 10.24850/j-tyca-2020-03-06

phenomenon. This is due to the noise signal varies in a parabolic way with a minimum around the 'sweet spot' located 50 mm from the transducer. The receiver beams of the signal only converge at the sweet spot and in the divergence region, the size of the sampled zone away from the sweet spot is reduced. This generates a reduction in the data quality, however, in the region between approximately 43 and 61 mm beneath the transducer can usually be collected the most reliable velocity information (Thomas, Schindfessel, McLelland, Creëlle, & De Mulder, 2017).

Other research works indicate that the sweet spot is located approximately 52 mm in the zone below the transducer, where the overlapping region of the acoustic beams of the ADV is the largest (Koca, Noss, Anlanger, Brand, & Lorke, 2017). Therefore, it is concluded that it is necessary to select the spot with lower noise signal, which corresponds to a local minimum.

Owing to that, a data filtering is applied in the turbulence intensity curves by selecting the local minimums of each profiling to make a representative graph of the phenomenon.

Calculation of the power coefficient using experimental data

A load cell of 9.806 N, whose measurement accuracy is 0.00196 N, was used to measure the hydrodynamic thrust on the discs since it receives the thrust from the disc using a stem joined to a sliding car (see Figure 8). The measurements were made in the three porous discs; and in the

Tecnología y ciencias del agua, ISSN 2007-2422, 11(3), 190-235. DOI: 10.24850/j-tyca-2020-03-06

case of the thrust measurement, five repetitions were made, being a total of 17 010 samples for each measurement.

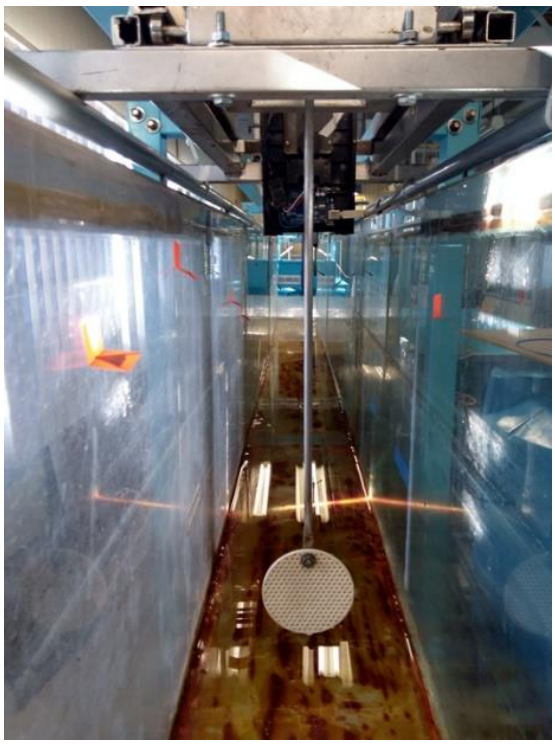

Figure 8. Device to measure the hydrodynamic thrust on a porous disc.

The net thrust in the discs was obtained by resting the stem thrust from the total ensemble (stem and disc).

On the other hand, the thrust coefficient is calculated using the equation (18), according to Harrison, Batten, Myers, and Bahaj (2010).

$$C_T = \frac{F}{0.5\rho u_0^2 A} \tag{18}$$

An approximate calculation of β was determined using the one-dimensional theory proposed by Houlsby *et al*. (2008) due to difficulties

Tecnología y ciencias del agua, ISSN 2007-2422, 11(3), 190-235. DOI: 10.24850/j-tyca-2020-03-06

to measure the mean velocity in the zone where the porous disc is located u_1, inasmuch as the acoustic Doppler velocimeter used presents limitations. Thus, the values of the respective axial induction factor a and β were determined after having estimated the value of C_T, and then the power coefficient was calculated.

Results and discussion

Experimental tests with various blockage ratios

The mean turbulence intensity in the section where the discs are located, which is representative of the channel, was determined using data of the velocities profiling in the vertical direction. For the tests with no porous disc submerged gave a mean value of 5.70%. A contours map of turbulence intensity is shown in Figure 9 for the cross-section of the channel, where were placed the porous discs. The values obtained are close to 8%, both in the bed of the channel and in the part of the free surface.

Tecnología y ciencias del agua, ISSN 2007-2422, 11(3), 190-235. DOI: 10.24850/j-tyca-2020-03-06

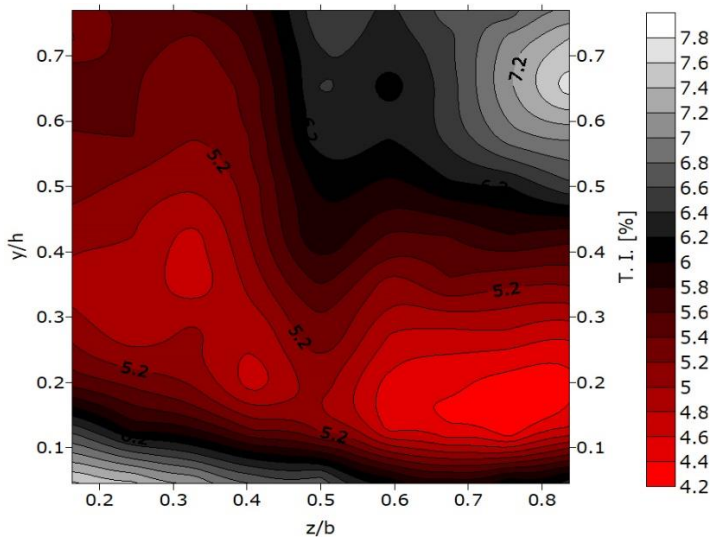

Figure 9. Turbulence intensity in the section of the channel where are located the porous discs (no disc).

Recovery of velocity and turbulence intensity in the channel with a porous disc of D_1 = 92.0 mm in diameter and a blockage ratio B_1 = 0.090

The results of measurements of the velocity profiles are shown in Figure 10 for x/D = 3, 6, 9, 12 and 15 downstream from the porous disc, including the velocity profile with no disc submerged in the fluid.

Tecnología y ciencias del agua, ISSN 2007-2422, 11(3), 190-235. DOI: 10.24850/j-tyca-2020-03-06

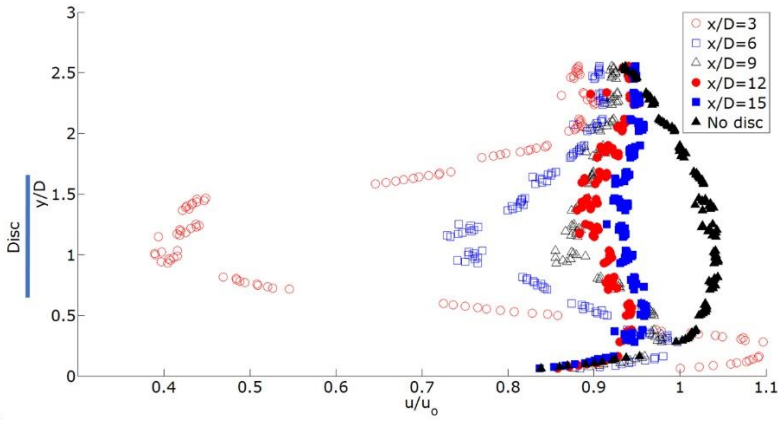

Figure 10. Velocity profiles for x/D = 3, 6, 9, 12, and 15 downstream from the porous disc, including the velocity profile with no disc submerged. Porous disc of 92.0 mm in diameter and blockage ratio B_1 = 0.090.

A velocities contours map was generated with the data of the velocity profiles measured in the vertical direction (Figure 11). The velocity recovery in x/D = 3 is 40% and for x/D = 12 is 90%, taking into account the values of the points located at the center of the disc, with respect to the bed of the channel y/D = 1.15.

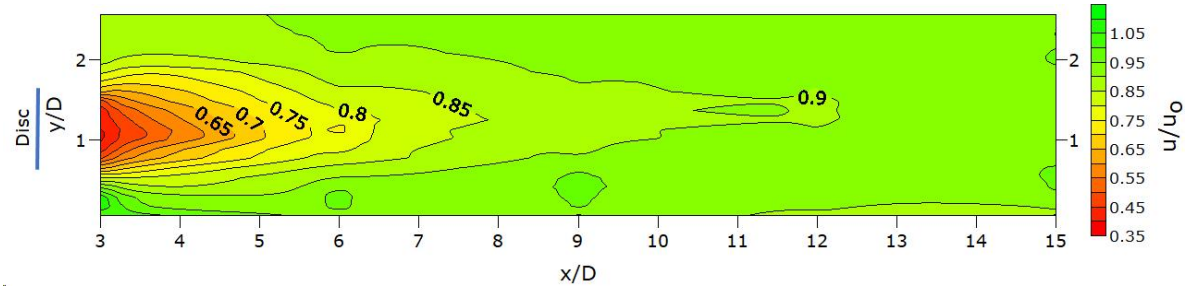

Figure 11. Velocity contours map. Porous disc of 92.0 mm in diameter and blockage ratio B_1 = 0.090.

Tecnología y ciencias del agua, ISSN 2007-2422, 11(3), 190-235. DOI: 10.24850/j-tyca-2020-03-06

The intensity turbulence profiles in the channel for x/D = 3, 6, 9, 12 and 15 downstream from the porous disc, including the turbulence intensity profile with no disc submerged in the fluid are shown in Figure 12. We can see in the figure that the superposition of the series of profiling generated with the data obtained using the acoustic Doppler velocimeter ADV presents some patterns that do not correspond to that expected in the physical phenomenon.

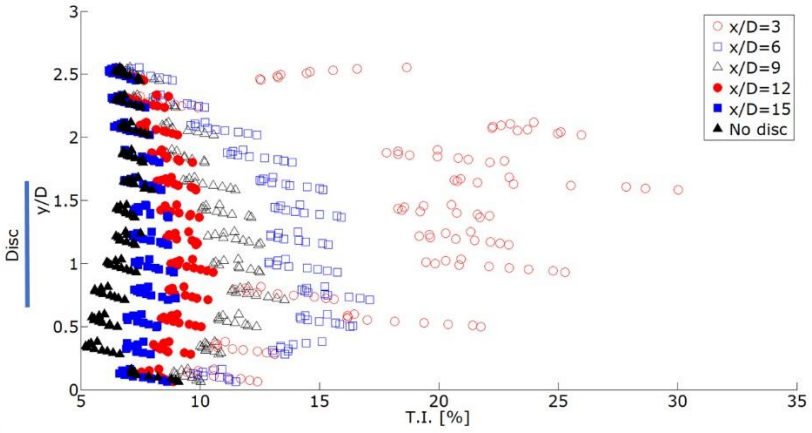

Figure 12. Turbulence intensities for the velocity profiles in the channel in x/D = 3, 6, 9, 12 and 15 downstream from the porous disc, and with no disc submerged. Porous disc of 92.0 mm in diameter and blockage ratio B_1 = 0.090.

Graphs shown in Figure 13 are generated by applying the data filtering to the profiles of turbulence intensity.

Tecnología y ciencias del agua, ISSN 2007-2422, 11(3), 190-235. DOI: 10.24850/j-tyca-2020-03-06

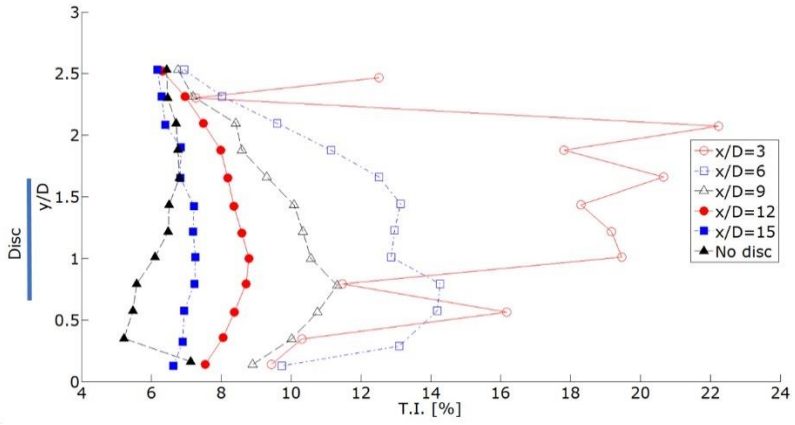

Figure 13. Data filtering applied to the turbulence intensities for the velocity profiles in the channel in x/D = 3, 6, 9, 12 and 15 downstream from the porous disc, and with no disc submerged. Porous disc of 92.0 mm in diameter and blockage ratio B_1 = 0.090.

The turbulence intensity at the center of the disc y/D = 1.15 presents values in x/D = 3 close to 20% and for x/D = 12, the values are approximately of 8%, being in general the highest values of turbulence intensity in each profile of velocities measured (Figure 14).

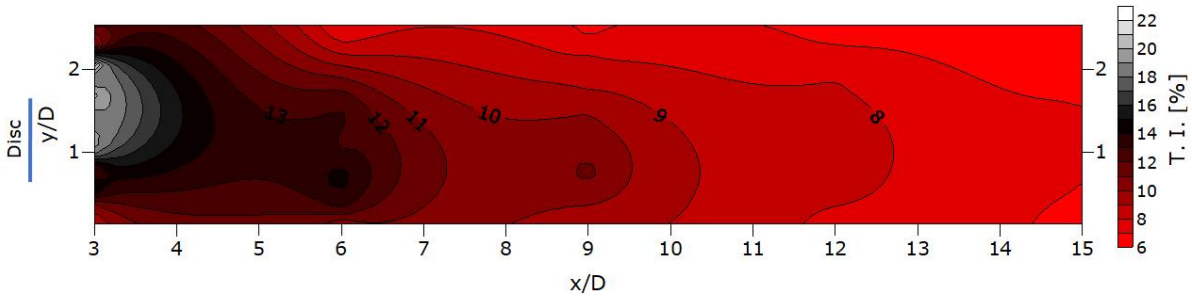

Figure 14. Contours map of turbulence intensity. Porous disc of 92.0 mm in diameter and blockage ratio B_1 = 0.090.

Tecnología y ciencias del agua, ISSN 2007-2422, 11(3), 190-235. DOI: 10.24850/j-tyca-2020-03-06

Recovery of velocity and turbulence intensity in the channel with a porous disc of D_2 = 120.8 mm in diameter and a blockage ratio B_2 = 0.156

The results of measurements of the velocity profiles in x/D = 3, 6, 9, 12 and 15 downstream from the porous disc are shown in Figure 15, including the velocity profile with no disc submerged in the fluid.

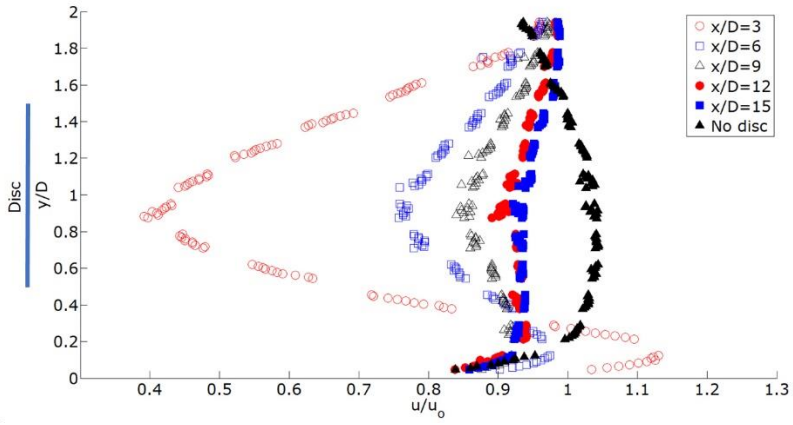

Figure 15. Velocity profiles for x/D = 3, 6, 9, 12, and 15 downstream from the porous disc, including the velocity profile with no disc submerged. Porous disc of 120.8 mm in diameter and blockage ratio B_2 = 0.156.

The velocity contours map generated with the measurements of the velocity profiles in the vertical direction is shown in Figure 16. For y/D = 1.0, which corresponds to the height of the disc center, the velocity recovery in x/D = 3 is 40% and for x/D = 12 the recovery obtained is 92%.

Tecnología y ciencias del agua, ISSN 2007-2422, 11(3), 190-235. DOI: 10.24850/j-tyca-2020-03-06

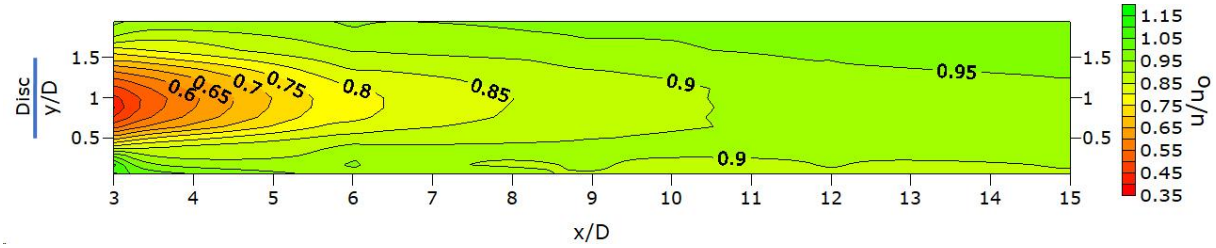

Figure 16. Velocity contours map. Porous disc of 120.8 mm in diameter and blockage ratio B_2 = 0.156.

The turbulence intensity profiles in the channel for x/D = 3, 6, 9, 12 and 15 downstream from the porous disc, including the turbulence intensity profile with no disc submerged in the fluid are displayed in Figure 17.

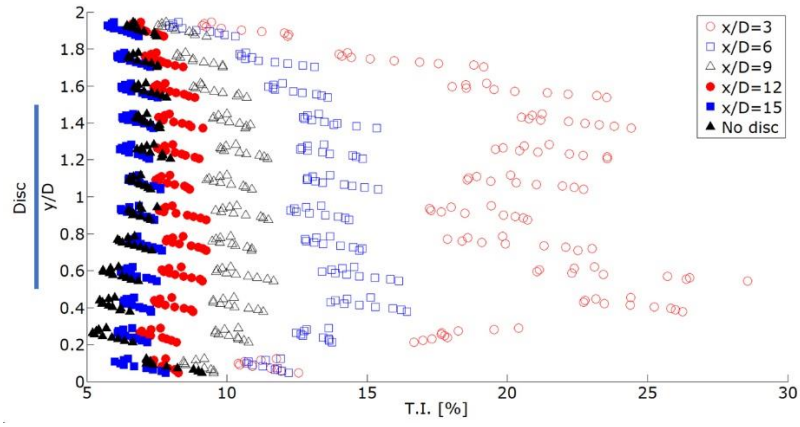

Figure 17. Turbulence intensities for the velocity profiles in the channel in x/D = 3, 6, 9, 12 and 15 downstream from the porous disc, and with no disc submerged. Porous disc of 120.8 mm in diameter and blockage ratio B_2 = 0.156.

Tecnología y ciencias del agua, ISSN 2007-2422, 11(3), 190-235. DOI: 10.24850/j-tyca-2020-03-06

The graphs shown in Figure 18 are generated by applying the data filtering to the turbulence intensity profiles.

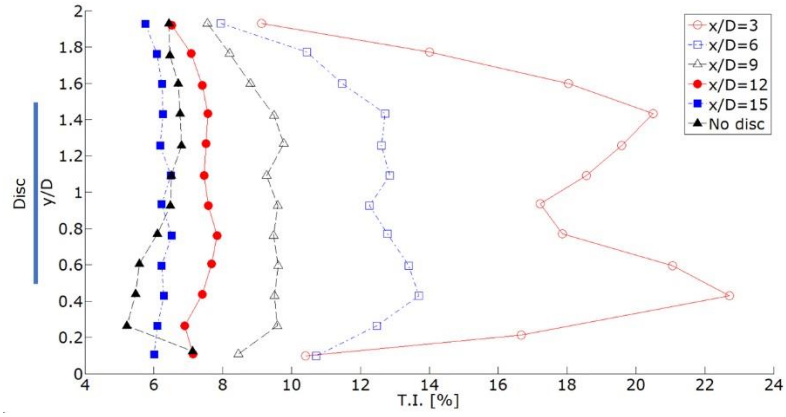

Figure 18. Data filtering applied to the turbulence intensities for the velocity profiles in the channel in x/D = 3, 6, 9, 12 and 15 downstream from the porous disc, and with no disc submerged. Porous disc of 120.8 mm in diameter and blockage ratio B_2 = 0.156.

In y/D = 1.0, where is the center of disc, the turbulence intensity presents values in x/D = 3 around 18% and for x/D = 12 around 8% (Figure 19).

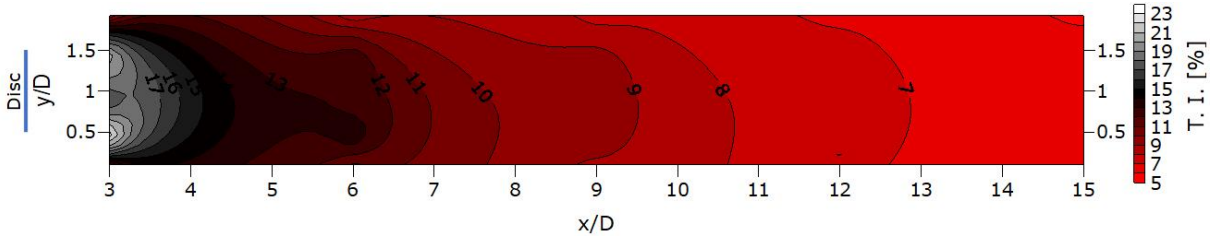

Figure 19. Contours map of turbulence intensity. Porous disc of 120.8 mm in diameter and blockage ratio B_2 = 0.156.

Tecnología y ciencias del agua, ISSN 2007-2422, 11(3), 190-235. DOI: 10.24850/j-tyca-2020-03-06

Recovery of velocity and turbulence intensity in the channel with a porous disc of D_3 = 135.7 mm in diameter and a blockage ratio B_3 = 0.197

The results of measurements of the velocity profiles for x/D = 3, 6, 9, 12 and 15 downstream from the porous disc are shown in Figure 20, including the velocity profile with no disc submerged in the fluid.

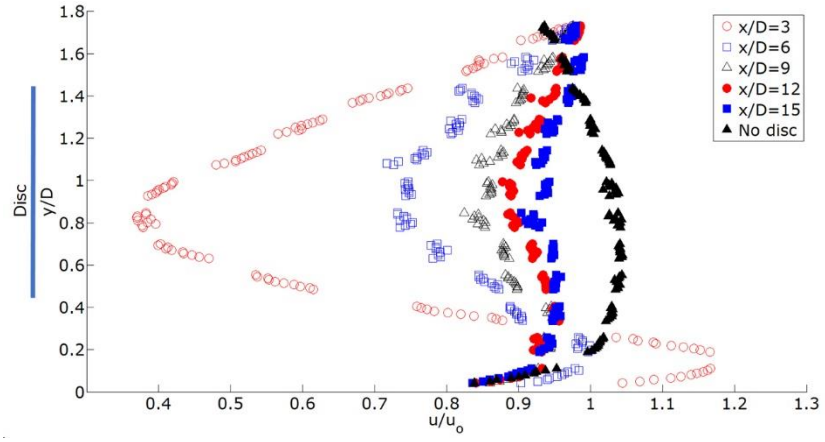

Figure 20. Velocity profiles for x/D = 3, 6, 9, 12, and 15 downstream from the porous disc, including the velocity profile with no disc submerged. Porous disc of 135.7 mm in diameter and blockage ratio B_3 = 0.197.

The velocities contours map was generated with the information of the velocity profiles in the vertical direction (Figure 21). Taking into account the points values located in y/D = 0.95, at the center of disc, the velocity recovery in x/D = 3 is 40% and for x/D = 12 gives 90%.

Tecnología y ciencias del agua, ISSN 2007-2422, 11(3), 190-235. DOI: 10.24850/j-tyca-2020-03-06

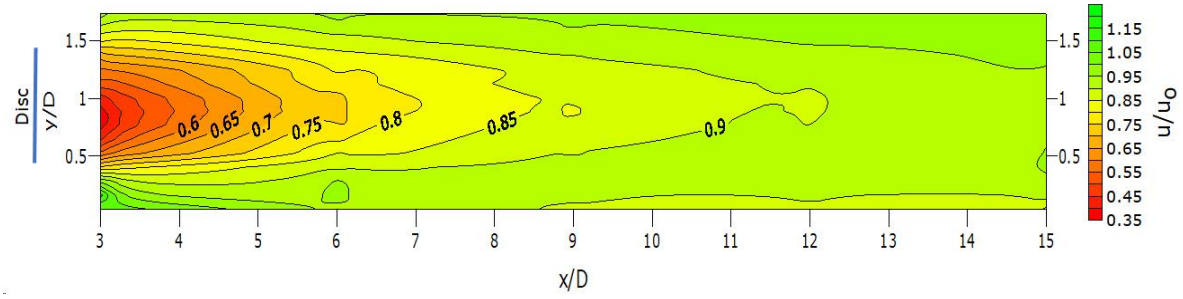

Figure 21. Velocity contours map. Porous disc of 135.7 mm in diameter and blockage ratio B_3 = 0.197.

The turbulence intensity profiles in the channel for x/D = 3, 6, 9, 12 and 15 downstream from the disc, including the turbulence intensity profile with no disc submerged in the fluid are displayed in Figure 22.

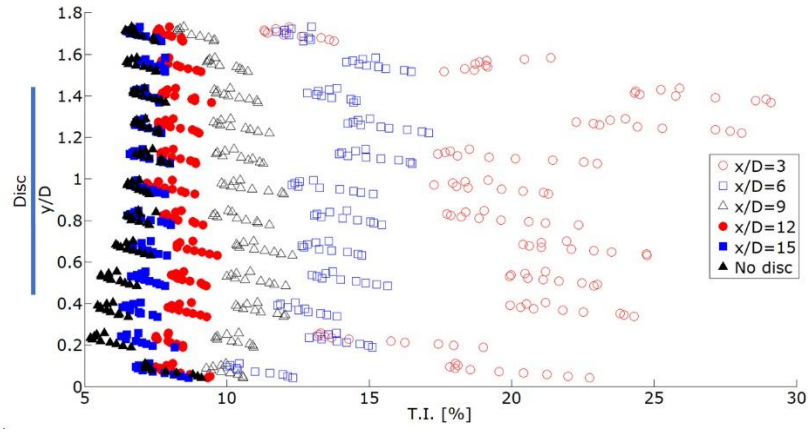

Figure 22. Turbulence intensities for the velocity profiles in the channel in x/D = 3, 6, 9, 12 and 15 downstream from the porous disc, and with no disc submerged. Porous disc of 135.7 mm in diameter and blockage ratio B_3 = 0.197.

Tecnología y ciencias del agua, ISSN 2007-2422, 11(3), 190-235. DOI: 10.24850/j-tyca-2020-03-06

The graphs shown in Figure 23 are generated by applying the data filtering to the turbulence intensity profiles.

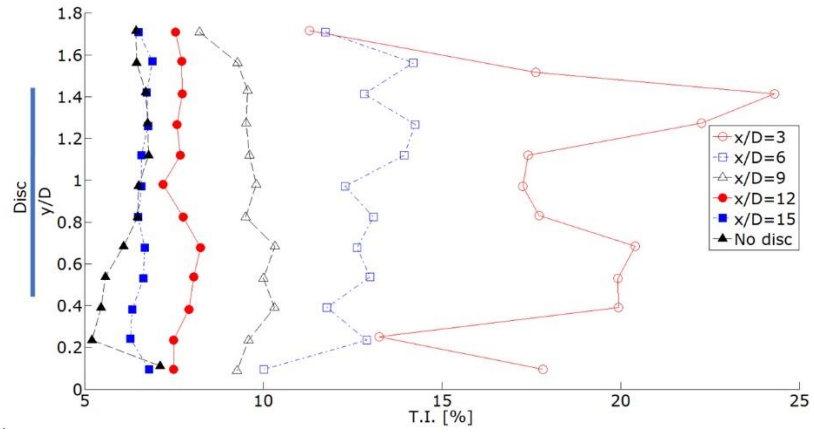

Figure 23. Data filtering applied to the turbulence intensities for the velocity profiles in the channel in x/D = 3, 6, 9, 12 and 15 downstream from the porous disc, and with no disc submerged. Porous disc of 135.7 mm in diameter and blockage ratio B_3 = 0.197.

The turbulence intensity presents values in x/D = 3 around 18% and for x/D = 12 around 8%, considering the points values located at the center of the disc y/D = 0.95 with respect to the channel bed (Figure 24).

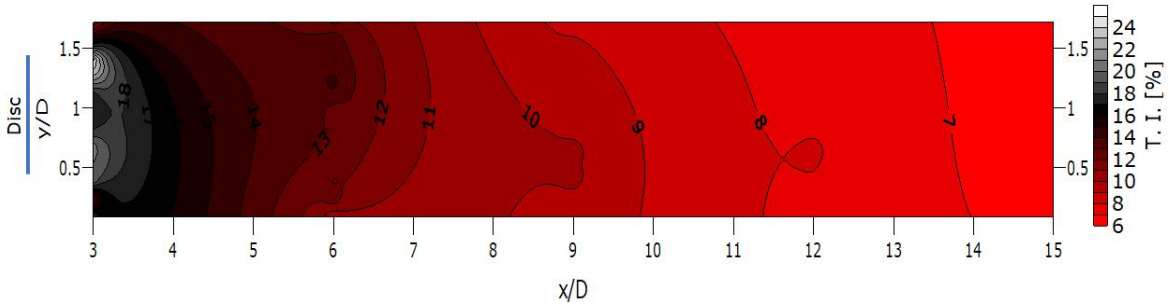

Figure 24. Contours map of turbulence intensity. Porous disc of 135.7 mm in diameter and blockage ratio B_3 = 0.197.

Tecnología y ciencias del agua, ISSN 2007-2422, 11(3), 190-235. DOI: 10.24850/j-tyca-2020-03-06

The results show mainly that for the hydraulic conditions established in the experimental channel, irrespective of the blockage ratio, the velocity recovery in the far wake at 12 diameters downstream from the disc reaches a close value to 90% respect to the mean velocity of the profile before introducing the discs. The same happens for the case of turbulence intensity, which at 12 diameters downstream from the disc shows a close value to 8%. This would enable to make a first recommendation for the optimum use of space of a hydrokinetic turbines row placed in series.

It is worth noting that the studies with high blockage ratios must be extended analyzing hydrokinetic turbines arrays as is common find them in canals and rivers. It is expected a rise in the velocity recovery in the far wake as blockage ratio is increased in turbines, as it is shown in the works of Chime y Malte (2014) with turbines row placed in parallel. Under this scenario would be important to analyze the behavior of the turbulence intensity curves and determine the optimum separation between turbines.

Calculation of the thrust coefficient and power coefficient for blockage ratios $B_1 = 0.090$, $B_2 = 0.156$ and $B_3 = 0.197$

The results of the hydrodynamic thrust for various blockage ratios are shown in Table 4. The hydrodynamic thrust between the disc with blockage ratio $B_1 = 0.090$ and that of the blockage ratio $B_2 = 0.156$ presents a 99% increase and the hydrodynamic thrust between the disc

Tecnología y ciencias del agua, ISSN 2007-2422, 11(3), 190-235. DOI: 10.24850/j-tyca-2020-03-06

with blockage ratio B_1 = 0.090 and that of the blockage ratio B_3 = 0.197 presents a 170% increase.

Table 4. Hydrodynamic thrust in porous discs with blockage ratios B_1 = 0.090, B_2 = 0.156 and B_3 = 0.197, experimental results.

Diameter of disc mm	Blockage ratio	Porosity	Total thrust N		Thrust on stem N	Thrust on disc N	
92.0	0.0904	0.34	1.448	±0.040	0.103	1.346	±0.040
120.8	0.1564	0.34	2.767	±0.049	0.088	2.679	±0.049
135.7	0.1976	0.34	3.719	±0.067	0.081	3.638	±0.067

The results of thrust and power coefficients are indicated in Table 5 for the various blockage ratios under study. The thrust coefficient between the disc with blockage ratio B_1 = 0.090 and that of the blockage ratio B_2 = 0.156 presents a 15% increase, while the thrust coefficient between the disc with blockage ratio B_1 = 0.090 and that of blockage ratio B_3 = 0.197 presents a 26% increase. On the other hand, the power coefficient between the disc with blockage ratio B_1 = 0.090 and that of blockage ratio B_2 = 0.156 presents a 37% increase, and the power coefficient between the disc with blockage ratio B_1 = 0.090 and that of blockage ratio B_3 = 0.197 presents a 59% increase.

Table 5. Thrust coefficient in porous discs with blockage ratios B_1 = 0.090, B_2 = 0.156 and B_3 = 0.197, experimental results.

Diameter of disc mm	Blockage ratio	Porosity	Water density kg/m³	Thrust on disc N		Area of disc m²	u_o m/s	u_1 m/s	C_T	C_p
92.0	0.0904	0.34	998.2	1.346	±0.040	0.0066	0.503	0.192	1.603	0.613

Tecnología y ciencias del agua, ISSN 2007-2422, 11(3), 190-235. DOI: 10.24850/j-tyca-2020-03-06

120.8	0.1564	0.34	998.2	2.679	±0.049	0.0115	0.503	0.228	1.845	0.838
135.7	0.1976	0.34	998.2	3.638	±0.067	0.0145	0.503	0.244	2.013	0.977

A comparison between the power coefficients obtained with the experimental tests and the maximum power coefficients obtained with the one-dimensional theory is indicated in Table 6. The differences in the values obtained are of 19.45% for the case B_1 = 0.090, of 4.13% for B_2 = 0.156, and 0.84% for B_3 = 0.197.

Table 6. Power coefficients in porous discs with experimental results and maximum power coefficients obtained with the one-dimensional theory.

Diameter of disc mm	**Blockage ratio**	**Porosity**	**Experimental C_p**	**One-dimensional theory $C_{p\max}$**	**Difference %**
92.0	0.0904	0.34	0.613	0.732	19.45
120.8	0.1564	0.34	0.838	0.872	4.13
135.7	0.1976	0.34	0.977	0.985	0.84

The influence of the blockage ratio in the power coefficient in porous discs with experimental results and using the one-dimensional theory of the actuator disc proposed by Houlsby *et al*. (2008) is shown in Figure 25.

Tecnología y ciencias del agua, ISSN 2007-2422, 11(3), 190-235. DOI: 10.24850/j-tyca-2020-03-06

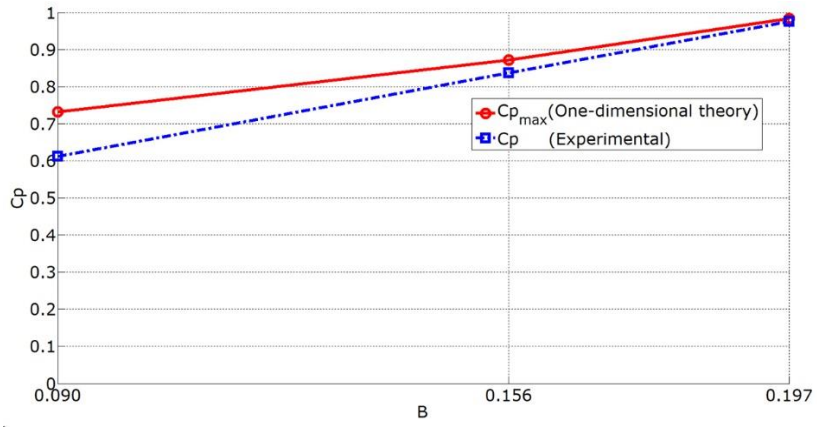

Figure 25. Power coefficient in porous discs with experimental results and maximum power coefficients obtained with the one-dimensional theory for various blockage ratios.

Conclusions

For various blockage ratios and the hydraulic conditions established in the experimental tests is concluded that the velocity recovery in the far wake, in *y*/*D* corresponds to the location of the center of the porous disc, reaches approximately 90% at 12 diameters downstream from the disc. The turbulence intensity at 12 diameters downstream from the disc presents a value around 8%, magnitude that for practical purposes is acceptable in comparison with 5.7% that exhibits the channel section with no porous disc. Thus, it is advisable to adopt this criterion to establish the minimum separation between one and other turbine when the row of turbines is placed in series.

According to the results obtained, it is observed an increase in the obtainable power of hydrokinetic turbines, when the blockage ratio in the canal is increased. For instance, increasing the blockage ratio from B_1 = 0.090 to B_2 = 0.156, the power coefficient increased by 37% and with an increase from B_1 = 0.090 to B_3 = 0.197, the power coefficient obtained rose by 59%.

By comparing the power coefficients C_{p1} = 0.613, C_{p2} = 0.838 and C_{p3} = 0.977, which were obtained for the blockage ratios B_1 = 0.090, B_2 = 0.156 and B_3 = 0.197, respectively, with the theoretical maximums expected, it was found that the power coefficient values are similar to the theoretical maximums expected with a blockage ratio of 0.20, and such coefficient declines by around 20% with respect to the theoretical maximum expected with lower blockage ratio values than 0.10.

Nonetheless, it is important acknowledge that in order to generalize the previous results, it is necessary to conduct more experimental tests in channels of several dimensions and using discs with different porosity too. The authors consider that the findings are sufficiently solid to have a first guidance when a decision is required to adopt the dimensions of a turbine and select the separation between turbines placed in series, especially whether to maximize the obtainable power is essential. Furthermore, it is desirable to carry out tests in canals with real conditions due to the roughness can be significant in the velocity profiles, or failing that, validate a physical-mathematical model with computational fluid dynamics CFD by using the results of this study, and thus to manipulate the variables of interest to generalize the results.

Tecnología y ciencias del agua, ISSN 2007-2422, 11(3), 190-235. DOI: 10.24850/j-tyca-2020-03-06

Acknowledgements

The authors express their gratitude to the Consejo Nacional de Ciencia y Tecnología de México (Conacyt) for the research grant given to carry out this study, as well as to the Universidad Nacional Autónoma de México (UNAM) and to the Instituto Mexicano de Tecnología del Agua (IMTA) for providing the facilities.

References

Garrett, C., & Cummins, P. (2007). The efficiency of a turbine in a tidal channel. *Journal of Fluid Mechanics*, 588, 243-251.

Goring, D. G., & Nikora, V. I. (2002). Despiking acoustic Doppler velocimeter data. *Journal of Hydraulic Engineering*, 128(1), 117-126.

Harrison, M. E., Batten, W. M., Myers, L. E., & Bahaj, A. S. (2010). A comparison between CFD simulations and experiments for predicting the far wake of horizontal axis tidal turbines. *IET Renewable Power Generation*, 4(6), 613-627.

Chime, A. H., & Malte, P. C. (2014). Hydrokinetic turbines at high blockage ratio. *Proceedings of the 2nd Marine Energy Technology Symposium*, METS2014, Seattle, WA, USA.

Houlsby, G. T., Draper, S., & Oldfield, M. L. G. (2008). *Application of linear momentum actuator disc theory to open channel flow (*Technical Report OUEL 2296/08). Oxford, UK: Department of Engineering Science, University of Oxford.

Koca, K., Noss, C., Anlanger, C., Brand, A., & Lorke, A. (2017). Performance of the vectrino profiler at the sediment-water interface. *Journal of Hydraulic Research*, 55(4), 573-581.

Lomelí, R., & Álvarez, N. (2014). La conservación de los distritos de riego y las cuencas de captación. *XXIII Congreso Nacional de Hidráulica*, Puerto Vallarta, Jalisco, México.

Maganga, F., Germain, G., King, J., Pinon, G., & Rivoalen, E. (2010). Experimental characterisation of flow effects on marine current turbine behaviour and on its wake properties. *IET Renewable Power Generation*, 4(6), 498-509.

Mori, N., Suzuki, T., & Kakuno, S. (2007). Noise of acoustic Doppler velocimeter data in bubbly flows. *Journal of Engineering Mechanics*, 133(1), 122-125.

Myers, L. E., & Bahaj, A. S. (2012). An experimental investigation simulating flow effects in first generation marine current energy converter arrays. *Renewable Energy*, 37, 28-36.

Okulov, V. L., & Van Kuik, G. A. (2012). The Betz-Joukowsky limit: On the contribution to rotor aerodynamics by the British, German and Russian scientific schools. *Wind Energy*, 15(2), 335-344.

Panton, R. L. (2005). *Incompressible flow.* New Jersey, USA: John Wiley & Sons, Inc. .

Thomas, R. E., Schindfessel, L., McLelland, S. J., Creëlle, S., & De Mulder, T. (2017). Bias in mean velocities and noise in variances and covariances measured using a multistatic acoustic profiler: The Nortek Vectrino Profiler. *Measurement Science and Technology*, 28(7).

Whelan, J. I., Graham, J. M. R., & Peiró, J. (2009). A free-surface and blockage correction for tidal turbines. *Journal of Fluid Mechanics*, 624, 281-291.

Xiao, H., Duan, L., Sui, R., & Rösgen, T. (2013). Experimental investigations of turbulent wake behind porous disks. *Proceedings of the 1st Marine Energy Technology Symposium*, METS2013, Washington, DC, USA.